

# Role of calcium and noise in the persistent activity of an isolated neuron

Simona Cocco

CNRS-Lab. Physique Statistique de l'ENS, 24 rue Lhomond, 75005 Paris, France.  
CNRS-Lab. Dynamique Fluides Complexes, 3 rue de l'Université, Strasbourg, France

(Dated: November 4, 2018)

The activity of an isolated and auto-connected neuron is studied using Hodgkin–Huxley and Integrate-and-Fire frameworks. Main ingredients of the modeling are the auto-stimulating autaptic current observed in experiments, with a spontaneous synaptic liberation noise and a calcium-dependent negative feedback mechanism. The distributions of inter-spikes intervals and burst durations are analytically calculated, and show a good agreement with experimental data.

Understanding the mechanisms responsible for persistent activity and rhythm settling is of central importance in neuroscience. The persistence of the activity is the neuronal basis of the working memory [1] and brains rhythms ranging from about 0.1 to 200 Hz have been recorded in sleep, waking and pathological states [2]. Such behaviors are usually network properties; for instance oscillations are possibly built on the existence of different e.g. inhibitory and excitatory populations of neurons [3]. From a theoretical point of view, the large number of neurons in networks allows the use of self-consistent (mean-field) methods to determine properties as the average spike emission frequency [4, 5, 6, 7, 8]. It was in particular found that a basis for persistent activity (with firing rate  $\sim 10 - 50$  Hz) is the ability of NMDA synaptic channels to integrate afferent inputs with a slow decay time constant ( $\sim 0.1$  s) [4].

Interestingly, persistence and rhythm settling have also been experimentally observed in systems made of an isolated and auto-connected excitatory neuron (autapse) [9]. Autapse are produced *in vitro* by grown excitatory neurons, extracted from rat embryos hippocampal, on coverslips [9, 10, 11]. Neurons normally develop up to 5 weeks and establish connections with themselves when no other neuron is nearby. The number of auto-connections increases with the age, as sketched in Fig.1. Patch pipettes allows both electrical recording of the neuronal activity and current injection to trigger spikes. After a spike has been triggered, more than 2 week old autapses carry on spiking in a whole burst of activity. Records show that both the time interval between successive spikes (ISI) and the duration of the burst (BD) fluctuate. Surprisingly, while the number of auto-connections increase with the age, the average spike frequency decreases (around 20, 5, 1 Hz for 2, 3, 4 week neurons respectively), see Fig.1. The neuron therefore exhibits a negative rate-control feedback mechanism preventing runaway excitations due to the strong, and growing with the age, positive auto-stimulating current. All those experimental results are reported in [9].

This letter presents a theoretical study allowing a quantitative interpretation of the autapse activity. Persistence is due to the interplay of two currents evidenced in experiments [9]: a small and slow postsynaptic com-

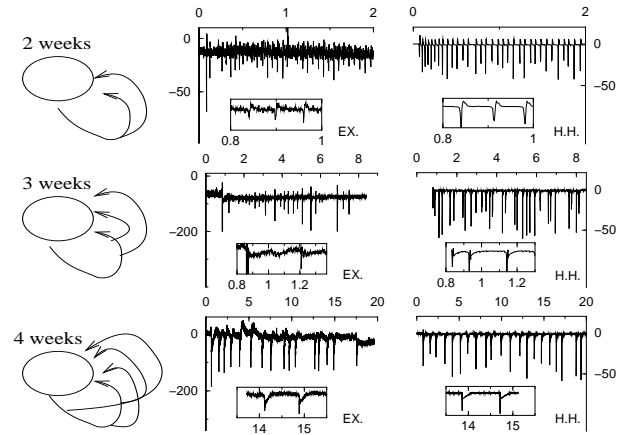


FIG. 1: Sketch of the autaptic system (left panel) showing the increase in synaptic connections with age (2, 3 and 4 weeks from top to down) and experimental (EX, middle) & theoretical (HH model, right) current time traces. Units are pA (EX) &  $\mu\text{A}/\text{cm}^2$  (HH) vs. seconds. Experimental data show bursts of activity for 3 representative neurons among 20 records. HH simulation show current dynamics for bursts of equivalent durations. Insets magnify two consecutive spikes chosen in the bursts, with typical ISI of 0.05, 0.2 and 1 s for 2, 3 and 4 weeks respectively. The autaptic AMPA current (negative *i.e.* inward, immediately after the spike) is very small and not visible at 2 weeks, large and observable at 3 weeks, huge at 4 weeks.

ponent and a random spontaneous synaptic liberation. To model rhythm settling, a calcium dependent negative feedback is introduced. This feedback is at the origin of spike frequency adaptation under an external current, previously modeled [12, 13] and experimentally observed in the autaptic system [11]. ISI and BD distributions are analytically calculated using an Integrate-and-Fire (IF) model, and compared to experimental data and numerical predictions from a detailed Hodgkin-Huxley (HH) model.

Currents in the autaptic system are represented in Fig 2. Pre-synaptic (spike) currents are introduced in HH through standard Sodium and Potassium gating variables [14, 15]; their modeling in IF is discussed below. The experimental characterization of the post-synaptic current [9] has evidenced three auto-stimulating components that follow the spike (Fig. 2):

1. A large amplitude excitatory AMPA component,  $I_{\text{AMPA}}$ , entering just (5 ms) after the spike, and rapidly

decaying. Its amplitude considerably increases with the age of the neuron, due to the growing number of connections (Fig. 1). The AMPA current is modeled, in HH, through an effective exponentially decreasing conductance [15]. We stress that the AMPA current arrival falls within the neuron refractory period and thus cannot by itself trigger a new spike; it however leads to a membrane potential depolarization (up to 0 mV), giving a bump in the flank of the spike in voltage records [9]. The AMPA depolarization has two consequences. It first slows down Na and K gating variable resets, increasing the refractory period. Secondly, it allows more calcium to enter the cell via voltage-gated channels, as soon as membrane potential exceeds -20 mV. In IF, AMPA, Na and K currents are altogether accounted for by the calcium  $Ca^{sp}$  entering at each spike, and the refractory period  $t_r$ . These two parameters (which depend on the age of the autapse) and the threshold  $\theta$  for spike firing are determined from the numerical analysis of HH [16], see Fig. 3 and [15].

2. A small amplitude and slow decaying component,  $I_D$ , due to NMDA and ICAN conductances [9].  $I_D$  depolarizes the membrane potential  $V$  during a burst to  $\sim -55$  mV; after the burst halts,  $V$  decays to the rest value  $V_l = -60$  mV with a time constant  $t_D$  ranging from 300 ms in young cells (2 weeks) to 1 s in mature cells (3 and 4 weeks). In both HH and IF,  $I_D$  is modeled as an exponentially decaying current,  $I_D(t) = I_D^0 e^{-(t-t_i-\delta t)/t_D}$ , released with a delay  $\delta t = 5$  ms after the spike occurring at time  $t_i$ ; the amplitude is set to  $I_D^0 = 2$  mA/cm<sup>2</sup>, and corresponds to a depolarization of the membrane potential of 5 mV.

3. A spontaneous and random synaptic release, called miniatures,  $I_S = g_s V s(t)$ . Both amplitude and frequency of the miniatures  $s(t)$  are stochastic [9]. The time interval between miniatures during a burst has been fixed to its average value  $\delta_s = 20$  and 10 ms for 2-3 and 4 week neurons respectively.  $\delta_s$  increases to its (much larger) rest value  $\sim 0.1$  s in about 5 s after the end of the burst. Release times are hence discrete and multiple of  $\delta_s$ , which makes the IF model mathematically tractable (taking into account the stochasticity in times between miniatures does not significantly affect the outcome [16]). The distribution  $P$  of the released amplitude  $\sigma$  is Poissonian; the mean  $m$  and the conductance  $g_s$  are fitted from experiments [17], and given in caption of Fig. 3. After release at time  $i \times \delta_s$ , the miniature exponentially decays,  $s(t) = (s^- + \sigma(i)) e^{-(t-i\delta_s)/t_s}$  with  $t_s = 5$  ms ( $< \delta_s$ ) from experiments. Parameter  $s^- = m/(e^{\delta_s/t_s} - 1)$  is the average residual amplitude before the release.

In addition, an inhibitory feedback due to the presence of a Calcium-dependent After Hyperpolarizing current,  $I_{AHP} = g_{AHP} \frac{Ca}{k_d} (V - V_K)$ , is introduced. Such a component is modeled as in [12] for HH and [4, 13] for IF. Parameters values are  $g_{AHP} = 5$  mS/cm<sup>2</sup>,  $V_K = -80$  mV,

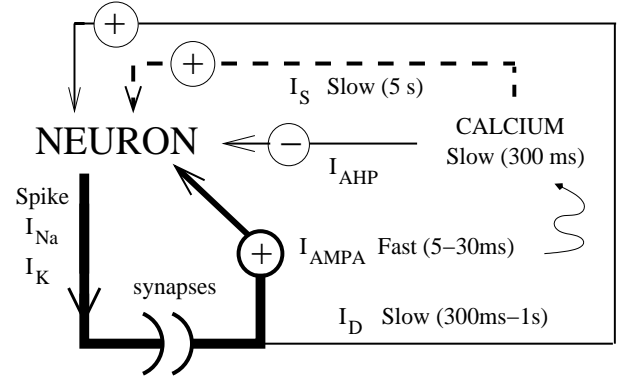


FIG. 2: Currents in the autaptic neuron model, with line widths proportional to amplitudes. Presynaptic currents  $I_{Na}$  and  $I_K$  accompany a spike. Postsynaptic components are, see text:  $I_{AMPA}$  (thick line), responsible for membrane depolarization and more Ca entering the cell (wiggly line);  $I_D$ , a slow depolarizing current (thin line);  $I_S$ , due to enhanced random spontaneous miniatures following Ca release (dashed line). The negative feedback is accounted for by a potassium hyperpolarizing current,  $I_{AHP}$ , with Ca-dependent amplitude.

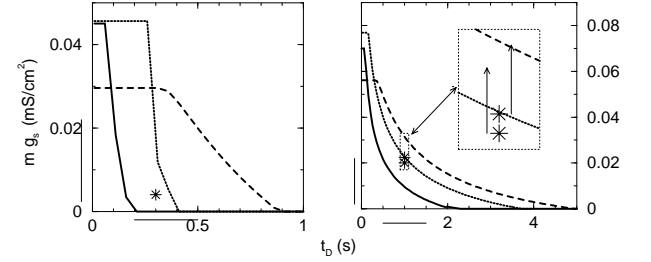


FIG. 3: Phase diagram for the persistence of activity in  $(t_D, m g_s)$  plane for  $g_l = 0.1, \theta = -53.5$  mV (left) and  $g_l = 0.2, \theta = -52$  mV (right). Bars symbolize ranges of experimentally observed values [9]. Parameters are:  $Ca^{sp} = 0.043$  (2 week, full), 0.115 (3 week, dotted) and 0.55  $\mu$ M (4 week neuron, dashed line). Activity persists above the lines, is absent below. Left: parameters, indicated by the star in (0.3, 0.004) with  $g_s = 0.002, m = 2$ , for a 2 week cell with stationary ISI of 0.07 s. Right: stars lies slightly below threshold at (1.0, 0.02) -  $g_s = 0.0032, m = 6.5$  (3 weeks) - and (1.0, 0.022) -  $g_s = 0.0032, m = 7$  (4 weeks). Positive fluctuations of the noise are needed for the activity to persist. Inset: magnification of the star-surrounding region; arrows indicate a positive standard deviation reaching (3 weeks: narrow line on the left) or (4 weeks: bold line on right) crossing the critical line. Average ISI are 0.2, 0.75 s for 3, 4 weeks respectively.

$k_d = 30 \mu$ M.

In the IF model, the dynamics of membrane potential  $V$  and calcium concentration  $Ca$  obey

$$C \frac{dV}{dt} = -I_l - I_{AHP}(Ca) + I_D - I_S \quad (1)$$

$$\frac{dCa}{dt} = Ca^{sp} \sum_n \delta(t - t_n) - \frac{Ca}{t_{Ca}} \quad (2)$$

where  $I_l = g_l (V - V_l)$  is the leak current,  $C = 1$  mF/cm<sup>2</sup>

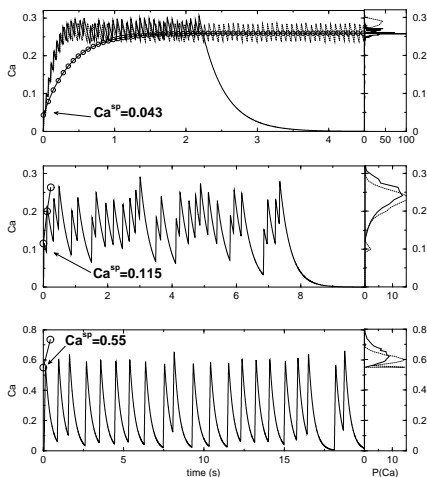


FIG. 4: From top to down, 2, 3 & 4 week neurons. Left: Calcium levels vs. time during a burst for random –HH, numerical, full line– and fixed amplitude –IF, theory, circles–miniatures. Jumps coincide with spikes. Right: IF –theory, full– and HH –numerical, dotted line– distributions of calcium right after spike emission. Distribution is very peaked for the 2 week neuron around  $Ca = 0.26$  (IF) and  $0.28$  (HH), and much wider due to noise-driven activity in older cells.

the capacity, and  $t_n$  the emission time of the  $n^{\text{th}}$  spike. A spike is fired when  $V > \theta$ , and the refractory period  $t_r$  is over. Large amplitude synaptic miniatures ( $I_S$ ) that add to the slow component ( $I_D$ ) can trigger a spike, provided the calcium-based inhibition ( $I_{AHP}$ ) is sufficiently weak. This mechanism is made possible by the fact that the slow component and high-frequency miniatures persist over a time period larger than (or, at least, equal to) the calcium decay constant  $t_{Ca} = 0.33$  s.

This few hundred ms time-scale is well separated from the integration time,  $\tau_m = C/g_l = 5 - 10$  ms for  $g_l = 0.1 - 0.2$ , and miniature decay time,  $t_s = 5$  ms. Consequently, once time  $t$  after the last spike emission is expressed in terms of miniature intervals,  $t = i \times \delta_s + \tau$ , where  $i (\geq 0)$  is integer-valued and  $\tau$  continuously ranges in  $[0; \delta_s]$ ,  $I_{AHP}$  and  $I_D$  do not vary with  $\tau$  [18]. From (2), the calcium level  $Ca$  is a function of its value  $Ca_-$  right after the previous spike and the interval  $i$ :  $Ca[Ca_-, i] = Ca_- e^{-i\delta_s/t_{Ca}}$ . We then integrate (1) analytically over  $\tau$  at fixed  $I_D(i)$ ,  $I_{AHP}(i)$ ,  $\sigma(i)$  and  $Ca_-$ . The resulting expression for the maximum of the membrane potential over  $\tau$ ,  $V_M(i, \sigma(i), Ca_-)$  [16], is then compared with  $\theta$ .  $i$  is increased by one if no spike is fired; otherwise, it is reset to 0 and the calcium level is increased by  $Ca^{sp}$ . Spike emissions (Fig. 1) are therefore reflected by jumps in the  $Ca$  level, as illustrated in Fig. 4.

Insights about the values of parameters allowing activity to be persistent can be obtained when considering first non-stochastic miniatures with fixed amplitude  $m$ . In this case, a stationary dynamics corresponding to a regular burst with infinite duration can settle down. The values for the calcium after each spike,  $Ca^*$ , and ISI,  $i^* \delta_s$ , are such that the calcium decrease

between two spikes balances the increase after a spike,  $Ca^* = Ca^{sp}/(1 - e^{-i^* \delta_s/t_{Ca}})$ . Inserting this result into the IF condition  $V_M(i^*, m, Ca^*) = \theta$  derived above yields a self-consistent equation for the stationary ISI value  $i^*$ . The existence or absence of solution to this equation indicates whether a persistent activity can be sustained or not [19]. The phase diagram is shown in Fig. 3, for two values of the neuron conductance,  $g_l = 0.1, 0.2$ , in the experimentally measured range.

The presence of noise in miniatures remarkably enriches this picture. Experimental features of ISI (average value in Fig. 1; small fluctuations for 2 week neurons and wide distribution for 3-4 weeks in Fig. 5) are well reproduced by parameters shown in Fig. 3. The system representative parameters (star) lies above the critical persistence activity line for 2 week cells, and slightly below for 3-4 weeks. In the latter case, miniatures showing positive fluctuations occasionally make representative parameters cross the phase border, and the neuron generates spike (noise-driven activity). On the contrary, in the former case, activity would persist forever in the absence of noise.

Finite burst duration results from a two-fold mechanism. On the one hand, if miniature amplitudes  $\sigma(i)$  happen to be lower than the minimal value that can trigger a spike in the vicinity of  $i^*$ , no spike will be fired. Later on, as the slow component decreases, spike firing becomes less and less likely. On the other hand, as a result of positive fluctuations in the  $\sigma$ s, a very short ISI may arise, making calcium increase and further spike firing unlikely.

The above results are illustrated in Fig. 4 for both HH/IF models, and noiseless/noisy dynamics. Note that, for 2 weeks neurons, persistent activity is possible in the absence of miniatures too ( $m = 0$ ) through the slow component only for 2 week cells. A burst, in the noisy dynamics, halts after a positive increase in calcium due to contiguous spikes with short ISI. For 3 and 4 week cells the noiseless IF dynamics does not reach stationarity, while the noisy dynamics results in finite and random duration bursts.

To calculate the stationary distribution of calcium, ISI, BD in presence of noise, we consider the probability  $\hat{T}(i|Ca_-)$  to fire with an ISI equal to  $i\delta_s$  given the calcium value  $Ca_-$  after the previous spike:  $\hat{T}(i|Ca_-) = \prod_{j=1}^{i-1} \bar{p}(j|Ca_-) (1 - \bar{p}(i|Ca_-))$ ;  $\bar{p}(j|Ca_-) = \sum_{k=0}^{s_m(j|Ca_-)-1} P(k)$  is the probability not to fire at interval  $j$  where  $s_m(j|Ca_-)$  is the minimal amplitude of noise able to trigger a spike at interval  $j$ ,  $P$  is the Poissonian with average  $m$ . The transition matrix between two successive calcium values read  $T(Ca|Ca_-) = \sum_i \hat{T}(i|Ca_-) \delta(Ca - Ca[Ca_-, i] - Ca^{sp})$ . The stationary calcium distribution,  $Q(Ca)$ , is the maximal eigenvector of  $T$ . We have discretized the calcium interval, and used Kelloggs iterative projection method to diag-

analyze  $T$  with the result shown in Fig. 4. The ISI distribution can be obtained from the matrix product of  $\hat{T}(i|Ca)$  and  $Q$ , and is shown in Fig. 5. It is very peaked around 0.05 (EX) - 0.06 (IF) s for 2 week cells, and spread out for 3 and 4 week neurons, with median 0.2, 0.75 s. respectively, in good agreement with experiments. To calculate the BD distribution, we define the generating function for the probability of an interval  $i \delta_s$  between spikes,  $G(x) = \sum_i Q(i)x^i$ . The coefficient of  $x^k$  in  $G(x)^n$ , denoted by  $[x^k]G(x)^n$  is the probability that a burst with  $n$  spikes has duration  $k \delta_s$ . Summing over  $n$ , we get the probability that a burst has duration  $k \delta_s$ ,  $[x^k]G(x)/(1 - G(x))$ . The resulting BD distribution is shown in Fig. 5; it decays as  $e^{-k/k_o}$  where  $k_o$  is the root of  $G(e^{1/k_o}) = 1$ . The agreement with experiments is good, even if comparison suffers from limited data (9, 13, 11 bursts for 2, 3, 4 weeks); it is excellent with HH simulation, which makes the analytical study of IF quite attractive despite the approximations done (discretization of time).

In conclusion, this letter proposes a possible mechanism that accounts for the persistence of activity in an isolated autapse. The slow current  $I_D$  sets the neuron in a depolarized 'up' state, also observed in various oscillatory networks [3] where it results from *e.g.* afferent inputs from other neurons. For 2 week neurons this up state can, by itself, sustain activity while, for 3 and 4 week, activity requires noisy synaptic liberation. Noise is at the same time responsible for persistent dynamics, robust with respect to changes of parameters [19], and the finite duration of bursts. The noise-driven mechanism for burst halting presented here differs from mechanisms based on a slow activity dependent depression [5] (either due to a modulation of cellular excitability, or to synaptic depletion [20]), and is supported by the observed large variability in burst durations. In addition, calcium-dependent spike frequency adaptation can explain the observed pattern of activity as the increase of ISI with the age. Finally, it would be interesting to extend the present study to the case of a network composed of a small number of similar neurons for which experimental data are available.

Acknowledgments: this work originates from discussions with C. Wyart, D. Chatenay and R. Monasson. I am particularly grateful to the latter for critical reading of the manuscript.

- 
- [1] D. Hebb, *The Organization of behavior* Wiley, New York, (1949).
  - [2] X.-J. Wang, Neural Oscillations in *Encyclopedia of Cognitive Science*, MacMillan Reference Ltd (2003).
  - [3] M.V. Sanchez-Vives, D.A. McCormick, *Nature Neurosci.* **3**, 1027 (2000).
  - [4] X.-J. Wang, *J. Neurosci.* **19**, 9587 (1999).

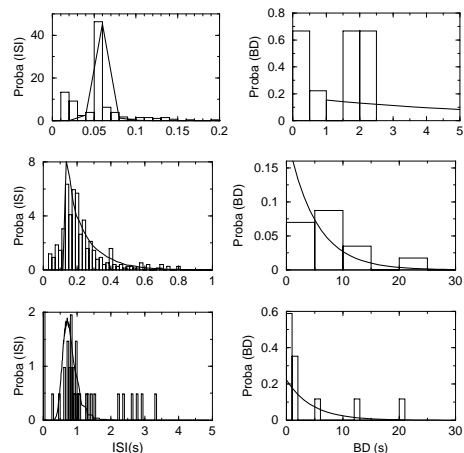


FIG. 5: ISI (left) and BD (right) distributions for 2, 3 & 4 weeks respectively (top to down). Histograms are experimental data, full lines are IF theoretical predictions. HH simulations, coinciding with IF predictions, are not shown.

- [5] J. Tabak, W. Senn, M.J. O'Donovan, J. Rinzel, *J. Neurosci.* **20**, 3041 (2000).
- [6] H.S. Seung, D.D. Lee, B.Y. Reis, D.W. Tank, *J. Comp. Neurosci.* **9**, 171 (2000).
- [7] A. Renart, N. Brunel, X.-J. Wang, in *Computational Neuroscience: A Comprehensive Approach*, J. Feng Ed., CRC Press, Boca Raton (2004).
- [8] D. Hansel, G. Mato, *Phys. Rev. Lett.* **86**, 4175 (2001).
- [9] C. Wyart, S. Cocco, J.F. Léger, C. Herr, L. Bourdieu, D. Chatenay, submitted to *J. Neurophysiol.* (2004).
- [10] J.M. Bekkers, C.F. Stevens, *Proc. Natl. Acad. Sci USA* **88**, 7834b (1991).
- [11] C. Wyart, C. Ybert, L. Bourdieu, C. Herr, C. Printz, D. Chatenay, *J. Neurosci. Methods* **117**, 123 (2002).
- [12] X.-J. Wang, *J. Neurophysiol.* **79**, 1549 (1998).
- [13] Y.H. Liu, X.-J. Wang *J. Comp. Neuroscience* **10**, 25 (2001).
- [14] A.L. Hodgkin, A.F. Huxley, *J. Physiol. (Lond)* **117**, 500 (1952).
- [15] Na and K dynamics parameters are borrowed from [12], with temperature constant  $\Phi_m = 1, \Phi_h = \Phi_n = 0.3$  and conductances  $g_{NA} = 3mS/cm^2, g_K = 1mS/cm^2$ . The amplitude and time constant for the AMPA component are fixed for 2, 3, 4 weeks to 0.1, 3, 20 in  $mS/cm^2$  and 10, 20, 30ms respectively [16]. The refractory period in the IF model is  $t_r = 10, 16, 85$  ms for 2, 3, 4 weeks.
- [16] S. Cocco, *in preparation* (2004).
- [17] Mean value and standard deviation of miniatures conductance in active neurons are  $g = 0.45$  nS,  $\sigma = 0.2$  nS respectively [9]. Fitting data with a Poissonian distribution [16] and writing  $g = g_0 m$ , we obtain  $m = g^2/\sigma^2 = 5$ ,  $g_0 = \sigma^2/g = .008$  nS, hence a conductance  $g_s = g_0/A = 0.002$  mS/cm<sup>2</sup> for a cell surface  $A = 4 \cdot 10^{-6}$  cm<sup>2</sup>.
- [18] J. Rinzel, G.B. Ermentrout, In: *Methods in Neural Modeling*, edited by C.Koch and I. Segev. Cambridge, M.A.: MIT Press, (1989) p. 135-170.
- [19] Even if a stationary solution exists, it may be not possible to reach for dynamical reasons *e.g.* for young neurons with special choices of parameters [16].
- [20] Synaptic depletion has been neglected here. Note that experimentally observed autaptic currents are not affected by repeatedly triggered spikes, except at very high stim-

ulation frequency  $\simeq 10 - 20Hz$  .